JOURNAL OF GEOPHYSICAL RESEARCH, VOL. 112, D23S90, doi:10.1029/2007JD009055, 2007

In situ measurements of aerosol mass concentration and radiative properties in Xianghe, southeast of Beijing

Zahra Chaudhry,[1] J. Vanderlei Martins,[2,3] Zhanqing Li,[1,4] Si-Chee Tsay,[5] Hongbin Chen,[6] Pucai Wang,[6] Tianxue Wen,[6] Can Li,[1] and Russell R. Dickerson[1]

Received 8 June 2007; revised 17 September 2007; accepted 22 October 2007; published 12 December 2007.

[1] As a part of the EAST-AIRE study, Nuclepore filters were collected in two size ranges (coarse, 2.5 μm < d < 10 μm, and fine, d < 2.5 μm) from January to May 2005 in Xianghe, about 70 km southeast of Beijing, and analyzed for aerosol mass concentration, spectral absorption efficiency and absorption coefficient. Twelve-hour aerosol mass concentration measurements showed an average concentration of 120 $\mu g/m^3$ in the coarse mode and an average concentration of 25 $\mu g/m^3$ in the fine mode. To determine how representative ground-based measurements are of the total column, the mass concentration data was compared with AERONET AOT at 500 nm and AERONET size distribution data. The vertical distribution of the aerosols were studied with a micropulse lidar and in the cases where the vertical column was found to be fairly homogenous, the comparisons of the filter results with AERONET agreed favorably, while in the cases of inhomogeneity, the comparisons have larger disagreement. For fine mode aerosols, the average spectral absorption efficiency equates well to a λ^{-1} model, while the coarse mode shows a much flatter spectral dependence, consistent with large particle models. The coarse mode absorption efficiency was compatible with that of the fine mode in the NIR region, indicating the much stronger absorption of the coarse mode due to its composition and sizable mass. Single scattering albedo results are presented from a combination between absorption coefficients derived from the filter measurements, from a PSAP and from a three-wavelength Nephelometer.

Citation: Chaudhry, Z., J. V. Martins, Z. Li, S.-C. Tsay, H. Chen, P. Wang, T. Wen, C. Li, and R. R. Dickerson (2007), In situ measurements of aerosol mass concentration and radiative properties in Xianghe, southeast of Beijing, *J. Geophys. Res.*, *112*, D23S90, doi:10.1029/2007JD009055.

1. Introduction

[2] According to the *Intergovernmental Panel on Climate Change* [2001], our ability to quantify the direct effect of aerosols on the global climate is hindered by uncertainties in the measurements of aerosol absorption. Both the sign and magnitude of the direct aerosol forcing at the top of the atmosphere are dictated by single scattering albedo, aerosol optical thickness, surface albedo, and phase function [*Coakley and Chylek*, 1975]. Rarely are pure aerosol types found in the atmosphere, as there are generally mixtures of different types, which further increases the complexity of quantifying the effect that aerosols have on local and regional climate [*Jacobson*, 2000]. Further knowledge is needed of both aerosol composition and vertical distribution, especially in the developing world.

[3] Various instruments such as the Integrating Plate [*Lin et al.*, 1973], Particle/Soot Absorption Photometer (PSAP, Radiance Research, Seattle, WA) [*Bond et al.*, 1999], Aethalometer [*Hansen et al.*, 1982] and other filter-based measurements have been used to obtain data on aerosol absorption. In cases where the vertical distribution of aerosols is fairly uniform, ground-based measurements are able to represent well the optical properties of aerosols in the total column. This is highly desirable, as ground-based measurements are relatively easy to acquire, cost-effective, and can offer relatively good spatial and temporal resolution.

[4] Remote sensing techniques such as satellites, lidar instruments and Sun photometers, such as the Aerosol Robotic Network, AERONET [*Holben et al.*, 1998], are better at measuring the total column amount of aerosols, and for gathering data on the vertical profile of aerosol optical properties, than most ground-based in situ instruments. Passive satellite remote sensing also offers excellent spatial

[1]Department of Atmospheric and Oceanic Science and the Earth System Science Interdisciplinary Center, University of Maryland, College Park, Maryland, USA.
[2]Department of Physics and Joint Center for Earth Systems and Technology, University of Maryland, Baltimore County, Baltimore, Maryland, USA.
[3]Also at NASA Goddard Space Flight Center, Greenbelt, Maryland, USA.
[4]Also at Institute of Atmospheric Physics, Chinese Academy of Sciences, Beijing, China.
[5]NASA Goddard Space Flight Center, Greenbelt, Maryland, USA.
[6]Institute of Atmospheric Physics, Chinese Academy of Sciences, Beijing, China.

0148-0227/07/2007JD009055$09.00

coverage, but, depending on the vertical structure of the atmosphere and surface reflectance, it has problems providing the aerosol concentration near the ground. The narrow swath of spaceborne lidars may provide good assessment of the vertical distribution of aerosols and clouds but do not provide global coverage like the passive instruments (e.g., CALIPSO [*Winker et al.*, 2003] and GLAS [*Zwally et al.*, 2002]). The drawback of column mean values is that they can mean very little to near-surface absorption if large concentrations of aerosols are in higher layers. Besides, collecting aerosol samples on the ground level also has the advantage of studying their impact on health as aerosols are a known health risk.

[5] The rapid population and economic growth seen in China over the last few decades has had strong effects on the local and regional air quality and climate. The increase in manufacturing and demand for products has led to serious air quality concerns. Several intensive studies have been conducted recently to examine the transport of air masses from the region over the Pacific, such as ACE-Asia [*Huebert et al.*, 2003] and INTEX-NA. The East Asian Study of Tropospheric Aerosols: an International Regional Experiment (EAST-AIRE) takes a closer look at the physical, optical and chemical properties of aerosols across China through a series of ground-based observation stations [*Z. Li et al.*, 2007]. One particular site, Xianghe, was chosen to host an Intensive Observation Campaign (IOC) during March 2005, when many instruments measuring the same parameters were run side by side to calibrate newer instruments against well-used and well-characterized instruments, as well as to ensure accurate measurements across various levels of resolution. The measurement site is detailed by *C. Li et al.* [2007]. For aerosol absorption, six instruments were run during this time period: 2 PSAPs, 3 Aethalometers and one sampling apparatus for collecting Nuclepore filters. This study will examine data from the Nuclepore filters and compare its absorption measurements against the University of Maryland's PSAP and the AERONET instrument.

[6] While other measurements of aerosol absorption allow for higher temporal resolution, the filter results allow for a more detailed spectral absorption analysis from 350–2500 nm. These results, in combination with the mass measurements, allow for the direct determination of the spectral mass absorption efficiency (in m^2/g), and for the study of individual particles using scanning electron microscopy. By collecting aerosol samples for 12 h, the day/night separation is preserved and the resulting Nuclepore filters have enough loading to be submitted for additional chemical composition analysis, such as ICPMS, PIXE or Ion Chromatography [*Ma et al.*, 2001; *Yamasoe et al.*, 2000]. Nuclepore filters offer a smooth surface for filter collection, reducing optical artifacts encountered with other filter types such as paper, Teflon and quartz [*Weiss and Waggoner*, 1984]. Particle collection on Nuclepore filters is also low-tech, using a simple sampling train, making it low-cost and ideal for field experiments.

[7] Other studies presented in this special issue address the issue of quantifying the aerosol radiative properties in Xianghe [*Z. Li et al.*, 2007]. *Zhao and Li* [2007] use spectral direct radiance measurements from an AERONET Sun photometer with total sky irradiance from a pyranometer to retrieve the single-scattering albedo. Their advantage is higher temporal resolution, on the order of 20 s, but they are limited to only cloud-free conditions, not usually an issue in this study. *C. Li et al.* [2007] examine aerosol radiative properties using a PSAP and a TSI three-wavelength Nephelometer, in association with many precursor gases measurements. Data from *C. Li et al.* [2007] is used in this study as a comparison with the filter measurements, and for the calculation of the average single scattering albedo throughout the filter sampling period. While the PSAP provides higher temporal resolution data than collecting filters, no upper end cutoff was used, possibly skewing the results with large particles.

[8] In this study, we present results of 5 months of sampling in Xianghe, China (39.798°N, 116.958°E; 35 m above sea level). Mass concentration measurements are presented in two size categories (coarse and fine) and compared with AERONET size distribution and AOT. The spectrally dependent absorption efficiency is measured and the absorption coefficient is calculated.

2. Methodology

[9] A two-stage sampling apparatus was installed at Xianghe, China in January 2005 to collect aerosol particles on Nuclepore filters. The system has an impactor inlet ensuring a 10 μm aerodynamic diameter cutoff size, and the impactor was coated with Apiezon grease to reduce particle bounce [*Hopke et al.*, 1997]. The first filter collected particles larger than 2.5 μm (hereafter referred to as the coarse mode) and the second filter collected particles less than 2.5 μm aerodynamic diameter (hereafter referred to as the fine mode) [*John et al.*, 1983]. Size-resolved filters were collected twice daily up to and through the IOC (January–March) and collected once daily for the next 2 months (April and May), with a few gaps due to instrument or supply-related problems. From January through March, the filters were changed between 0600 and 0700 LT and between 1900 and 2000 LT. The initial flow through the filters was set at 18 lpm manually and only filters with a final flow of greater than 8 lpm were analyzed. The instantaneous flow rate was recorded in a data logger and utilized in data analysis to correct for flow changes during the sampling.

[10] The filters were subjected to gravimetric analysis prior to and after field deployment. Blank filters were sent to the field among the exposed filters and were treated similarly to monitor the whole process. The filters were exposed to an ionizer for 24 h prior to weighing to remove static charge and to ensure an accurate weight measurement. The humidity in the ionizing chamber was recorded for each cycle and maintained around 20%. The humidity of the weighing room was also recorded at around 40%. The difference in humidity was determined not to affect the particles on the filters. Since the particles were collected at a variety of humidity levels, but analyzed dry, the higher humidity of the weighing room was not great enough to rehumidify the particles. According to meteorological data at the measurement site in Xianghe, the local humidity level stayed relatively low, averaging 36% during the IOC [*C. Li et al.*, 2007].

[11] After gravimetric analysis, the filters were subjected to an optical reflectance (OR) technique previously applied by *Martins et al.* [1998], and validated against an extinction

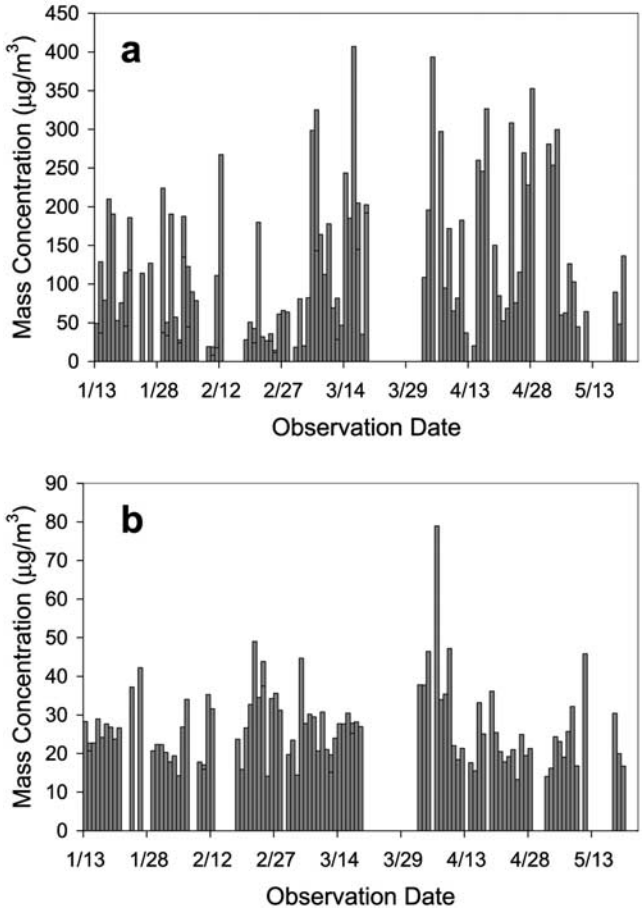

Figure 1. Twelve-hour mass concentration of (a) coarse mode particles with aerodynamic diameter 2.5 μm < d < 10 μm and (b) fine mode particles with d < 2.5μm for the period between 13 January and 24 May 2005 in Xianghe, China.

cell and Nephelometer measurements by *Reid et al.* [1998]. The filter is placed on a diffusive Spectralon panel and illuminated from above. The amount of light reflected is measured from 350 nm to 2500 nm by an ASD (Analytical Spectral Devices, Boulder, Colorado) LabSpec Pro spectrometer, with radiometric stability of 1% and precision of approximately 3% [*Kindel et al.*, 2001]. By passing light through the particles and reflecting the light off the filter and the Lambertian surface below, we are essentially mimicking the same method used by satellite sensors, with the advantage that we can characterize well the bright surface underneath the particles. Blank filters were also placed on top of the Spectralon panel and measured as a reference for the reflectance method. Since the aerosol particles were collected on the surface of Nuclepore filters, we expect fewer optical artifacts with this method than with particles collected inside the fibers of quartz, Teflon or paper filters [*Clarke*, 1982]. The main optical artifacts observed on particles collected on the surface of Nuclepore filters come from an increased proximity between particles as a function of filter loading. The interaction between close particles and the fact that they are touching the surface of the filter produce nonlinearities in the Beer-Lambert Law which can be modeled by a power law function. A calibration curve of this power law using artificial absorbing particles with known optical properties and a variety of mass loading is presented by J. V. Martins et al. (Spectral absorption properties of urban aerosol particles from 350–2500 nm, submitted to *Geophysical Research Letters*, 2007, hereinafter referred to as Martins et al., submitted manuscript, 2007).

[12] The light attenuation by absorbing particles and the mass concentration are used to determine the spectral absorption efficiency (m^2/g). The spectral absorption efficiency can be combined with the mass concentration measurement ($\mu g/m^3$) to obtain the absorption coefficient (m^{-1}). *Martins et al.* [1998] show results for black carbon mass absorption efficiency (α_{bc}) whereas here we show the aerosol mass absorption efficiency (α_a), where the absorption coefficient measured from the reflectance technique is divided by the total aerosol mass instead of the black carbon mass. The absorption coefficient was calculated from the filters by utilizing the OR absorption efficiency at 550 nm and was compared with PSAP results at 574 nm, which was operated in parallel with the filter sampling apparatus. The 550 nm wavelength was chosen to compare with the three-wavelength Nephelometer used during the IOP. Data from the University of Maryland's PSAP was obtained corresponding to the IOP at 5-min intervals, corrected according to *Bond et al.* [1999], and extrapolated to 550 nm following *Virkkula et al.* [2005]. The University of Maryland's instruments are detailed by *C. Li et al.* [2007]. Since the filters were collected over approximately 12-h intervals, the PSAP data were averaged over the same time period as the corresponding filter. The PSAP averages were also weighted according to the flow through the filter to account for the decrease in flow throughout the sampling period. This procedure ensured that both instruments sampled the aerosols similarly. This same process of averaging and weighting was applied to data obtained from the University of Maryland's three-wavelength TSI Nephelometer. The single scattering albedo (ω_0) was calculated using the absorption coefficient from the PSAP and from the OR and the scattering coefficient from the Nephelometer at 550 nm. The PSAP and Nephelometer were deployed on the same observatory tower as the filter sampling apparatus, but they did not include an upper limit cutoff size like the 10 μm inlet used for the filters [*C. Li et al.*, 2007].

3. Results and Discussion

3.1. Mass Concentration

[13] The mass concentration of the particles was determined by gravimetric analysis and by the measured air volume sampled in each filter. The mass concentration of the coarse particles (2.5 μm < d < 10 μm) from 13 January to 24 May 2005 is shown in Figure 1a. During this time period, values ranged from 8 to 407 $\mu g/m^3$ in the coarse mode with an average concentration of 120 $\mu g/m^3$. The mass concentration of the fine particles (d < 2.5 μm) is shown in Figure 1b, where the values ranged from 10 to 79 $\mu g/m^3$ with an average concentration of 25 $\mu g/m^3$. Other studies to measure aerosol mass concentration in China have found similar results. *Bergin et al.* [2001] measured daily mean PM2.5 concentrations of 136 $\mu g/m^3$ with a standard deviation of 48 $\mu g/m^3$ during one week in June 1999 in Beijing, which expectedly shows higher concentrations than at Xianghe, which is in a

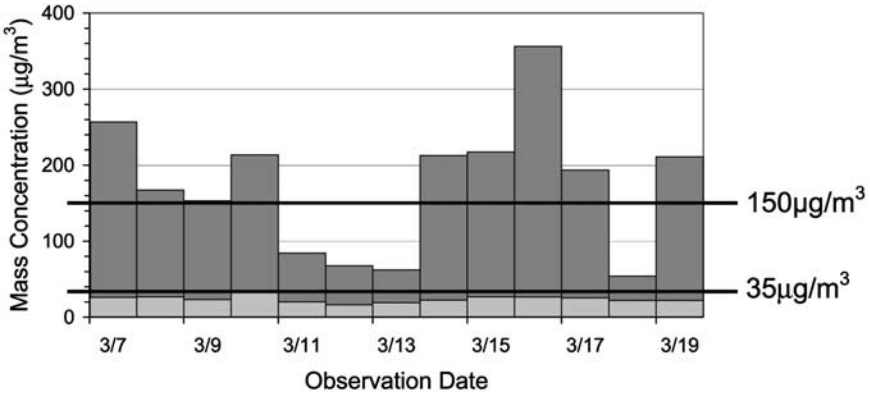

Figure 2. Twenty-four-hour averages of PM2.5 (light gray) and PM10 (total column) during the Intensive Observation Campaign compared to the US NAAQS 24-h limit for particulate matter.

relatively rural location. Also in Beijing, *Ning et al.* [1996] measured average total suspended particle (TSP) concentrations of 320 μg/m^3 in the summer and 680 μg/m^3 in the winter during 2 years (a) of measurements in 1986 and 1987. In another Chinese city, Shanghai, *Ye et al.* [2003] measured weekly PM2.5 mass concentrations ranging between 21 μg/m^3 and 147 μg/m^3 at two locations, with an annual average of 57.9 μg/m^3 and 61.4 μg/m^3 at each site, from March 1999 through February 2000. *Shi et al.* [2003] chose a suburban location, Nankou, a town 45 km northwest of central Beijing, to study mass concentration, similar to this study. The authors measured PM2.5 mass concentrations of 177 ± 53 μg/m^3 and PM10 mass concentrations of 334 ± 96 μg/m^3 during one week in March of 2001.

[14] From the mass concentration data during the IOC, which were separated in 12 h day and night samples, a 24-h average was calculated for PM2.5 and PM10. Here, PM10 is defined as the sum of the fine and coarse filter, which will account for all particles of d < 10 μm. The 24-h IOC PM10 and PM2.5 results are shown in Figure 2. To put the data in perspective, they are compared with the US EPA National Ambient Air Quality Standards (NAAQS). The 24-h average NAAQS limit for PM2.5 (35 μg/m^3) and for PM10 (150 μg/m^3) are shown in the plot. The PM2.5 limit was exceeded once during the IOC, at an average concentration of 35.4 μg/m^3 on 10 March 2005. The PM10 limit, however, was breached on 67% of the days of the IOC, and on those days averaged 47% greater concentrations than the NAAQS limit. Over the 5-month sampling period, the PM2.5 limit was exceeded 13% of the days, and the PM10 limit was exceeded 43% of the days. While PM10 is considered to be a lesser health risk than PM2.5, the respiratory problems, the visibility reduction, and the weather and climate impacts that arise from high concentrations of PM10 are still valid concerns.

[15] In addressing the aerosol radiative forcing of the climate and health issues related to aerosol pollution, a major challenge remains as to how well the total column mean properties of the aerosol retrieved from the ground (e.g., AERONET [*Holben et al.*, 1998; *Smirnov et al.*, 2000]) or from satellites (e.g., MODIS [*Kaufman et al.*, 1997; *Remer et al.*, 2002; *Ichoku et al.*, 2002; *Chu et al.*, 2002]) represent the mass concentration measurements or other observed aerosol properties at the ground level, or vice versa. The answer to this question has implications for the monitoring of aerosols from space and for the development of observation networks. The existence of aged versus fresh aerosol particles, or long-range transport of different aerosol types (e.g., dust transported over pollution aerosols), or any other source of inhomogeneity in the vertical aerosol distribution throughout the atmospheric column can affect this relationship. This possibility must be studied in different location and on a case-by-case basis.

[16] One way to compare the ground-based filter measurements to total column remote sensing is to look at AERONET-based retrievals of aerosol particle size distribution. Note that the size distribution data from AERONET are derived from the almucantar and principal plane scans, while the direct Sun measurement produces a quantity with superior uncertainty, the Aerosol Optical Thickness (AOT). Because of the heavy aerosol loading at Xianghe, many more direct Sun measurements were recorded than almucantar and principal planes. Since the filter samples were collected in two size ranges, fine and coarse, a direct comparison of the small mode ratio, SMR, can be per-

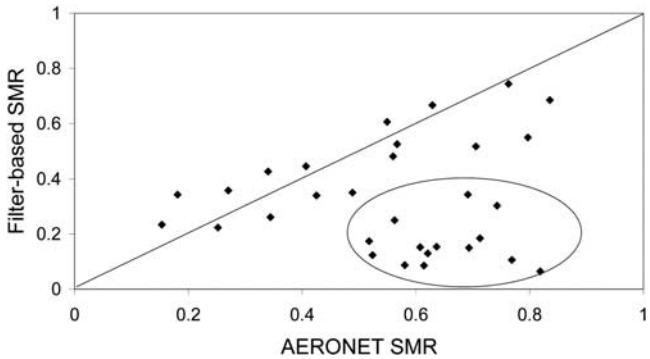

Figure 3. Comparison between calculated AERONET small mode ratio versus the measured filter small mode ratio for available data from 13 January to 24 May 2005. AERONET results were calculated from the average of almucantar inversions performed throughout the day, whereas the filter data was sampled during the daylight hours. The 1:1 line is shown in the plot to indicate cases of good agreement between both results. Cases of poorer agreement are circled.

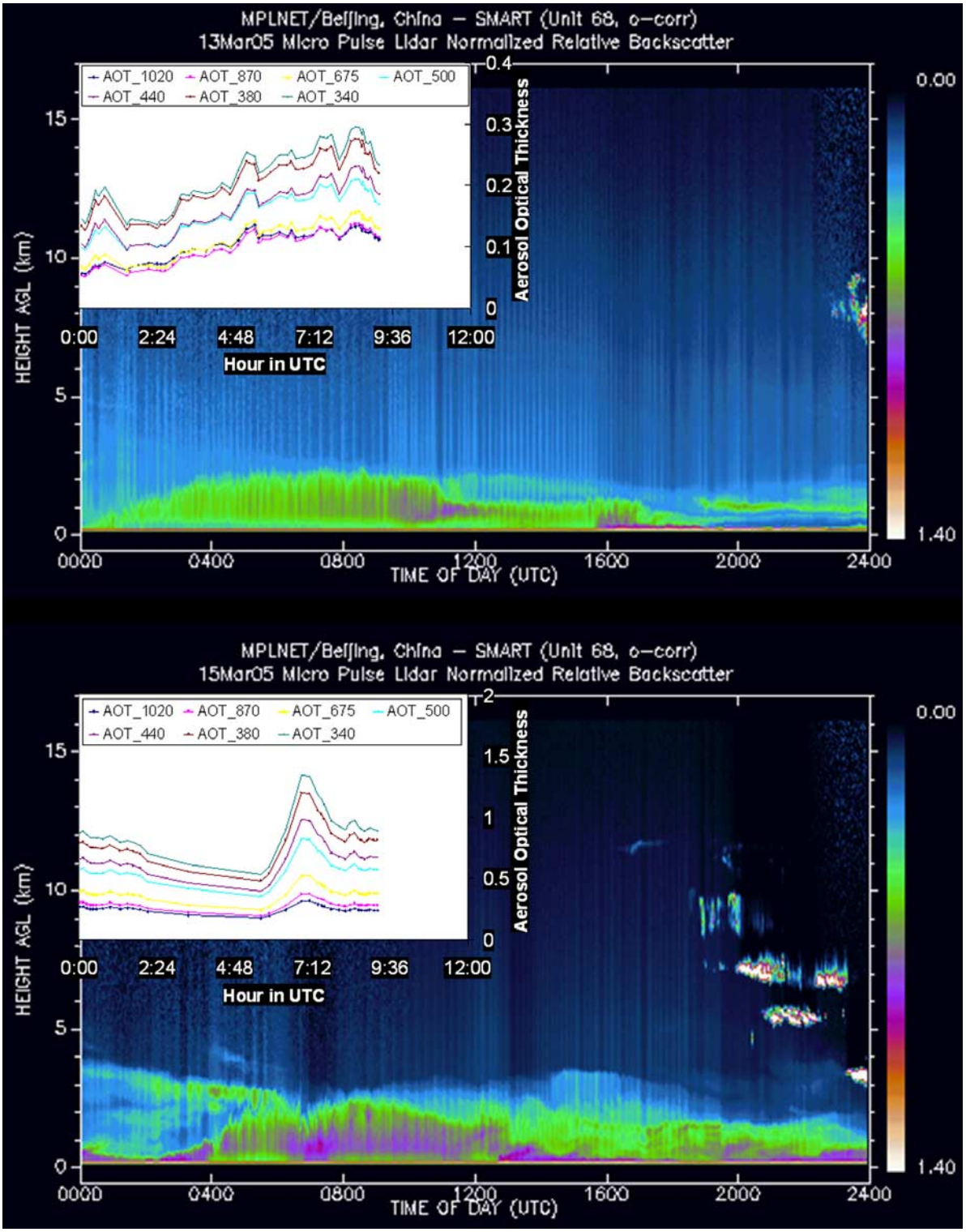

Figure 4. Lidar scan and corresponding AOD time series from AERONET for (top) 13 March 2005, representing one case when the calculated AERONET small mode ratio (SMR) and the filter SMR were correlated. The panel shows a relatively well mixed boundary layer during the AERONET data collection and the filter sampling period. (bottom) One case, 15 March 2005, when the calculated AERONET SMR and the filter SMR did not correlate well. The lidar image shows significantly heterogeneous layers during the sampling period.

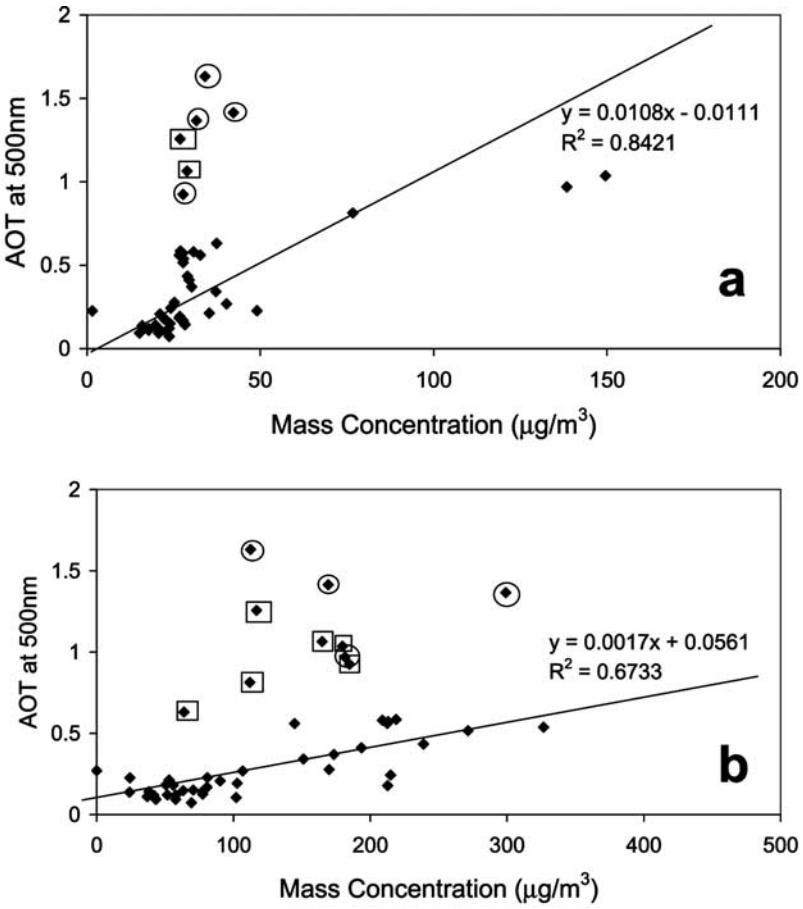

Figure 5. (a) Fine mode and (b) PM10 concentrations versus AERONET AOT at 500 nm. The marked points are not included in the correlation; circled points indicate lack of agreement from the SMR comparison in Figure 3 while points in squares indicate lack of AERONET size distribution data.

formed between the filter results and the AERONET total column almucantar retrievals. The filter SMR is calculated by dividing the daytime fine mode mass concentration by the total (fine + coarse) daytime mass concentration. The AERONET SMR comes from integrating the AERONET volume size distributions up to 2.24 μm diameter (the closest size bin constraint to 2.5 μm), and dividing by the total volume up to 10 μm diameter. The AERONET calculations assume the same mass density for the fine and coarse modes. Figure 3 shows a comparison between the SMR results of the filter versus AERONET. The 1:1 line indicated in the plot shows that there is one group of points with good agreement between both techniques and a second group (circled) where the AERONET results show consistently larger SMR, indicating smaller particles in the atmospheric column than near the ground.

[17] For the circled data points, one would assume that there was an external factor that did not allow the ground-based measurements to accurately represent the total column, usually in the case of aerosol layers aloft or diurnal changes within a relatively calm boundary layer. To test this hypothesis, data were used from NASA's MPLnet, as a micropulse lidar was located nearby. Lidar scans for the dates with good agreement between the filter SMR and AERONET SMR showed relatively uniform aerosol concentrations throughout the measurable vertical extent, as shown by a representative scan in Figure 4 (top) on 13 March 2005. The time series of AOT from AERONET was laid over the corresponding scan time period to determine if lidar backscatter variations were related to aerosol loading, not cloud contamination or sampling biases in AERONET due to selective cloud cover during portions of the day. Lidar scans for dates with poor agreement between the SMRs usually showed heavy aerosol layers aloft, or very inhomogeneous aerosol concentrations throughout the boundary layer, as seen in a representative scan in Figure 4 (bottom) for one case on 15 March 2005. On the basis of these results, we can say that the SMR data gathered by ground-based measurements are accurate representations of the total column in those instances when the total column is well mixed.

[18] Assuming a constant mass extinction efficiency (m^2/g), one can determine how well the AOT retrieved by an AERONET Sun photometer can represent the mass concentration measured on the ground. *Smirnov et al.* [2000] offer a similar comparison from Barbados, studying transported Saharan dust. Only quality-assured AERONET level 2.0 daily averages from the Sun photometer located in Xianghe were used for this comparison. Since the Sun photometer computes AOT from its direct Sun measurement, the daytime filters were selected instead of 24-h filters, as the Sun photometer can only collect data during daylight hours. In Figure 5a, the fine mode mass concentration is compared

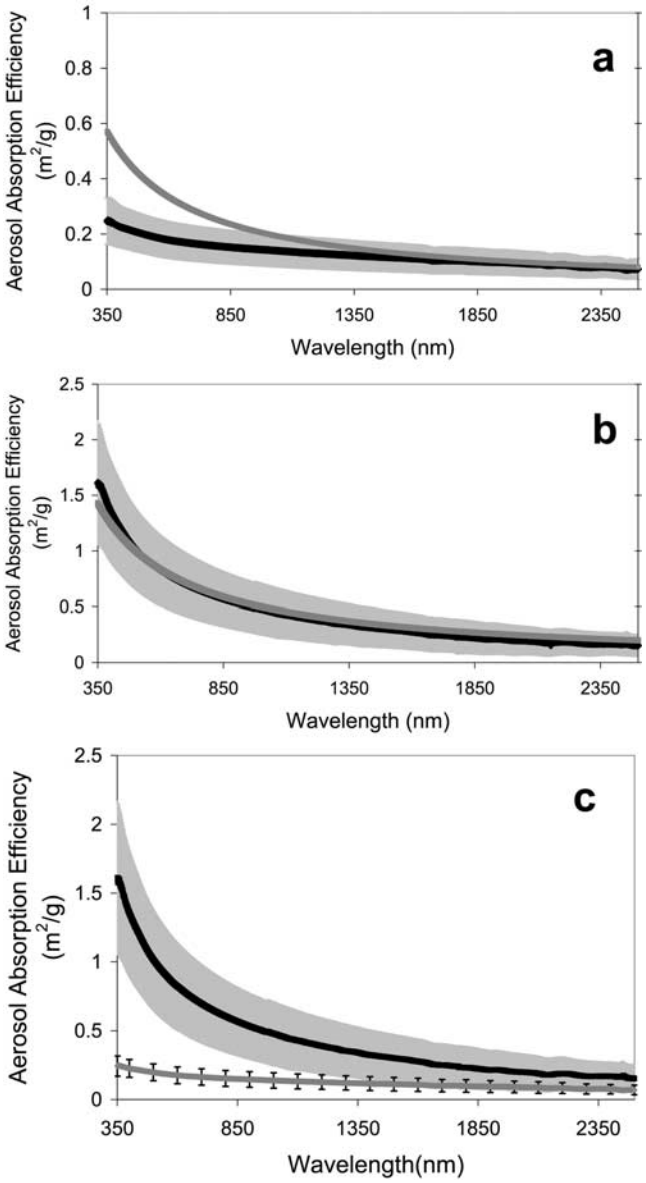

Figure 6. Spectral absorption efficiency (black line) for aerosol particles of (a) 2.5 μm < d < 10 μm and (b) d < 2.5 μm averaged from 35 filters from 3 to 19 March 2005 compared to a λ^{-1} model (gray line), then (c) compared to each other. The shaded area in each case represents the standard deviation of the measured cases. The error bars in Figure 6c are equivalent to the shaded area in the Figure 6a plot but are shown as error bars for visual clarity.

to AERONET AOT at 0.50 μm, while Figure 5b shows a similar comparison with PM10 concentrations. This particular wavelength was chosen for consistency, as it will be used throughout this paper. With help from the SMR comparison, we can identify two distinct paths taken by the data. The points surrounded by circles in Figure 5a show cases where the correlation in SMR were poor, while points in squares indicate dates when there is no AERONET size distribution data available. This result serves as a guide to filter the best cases in the intercomparison between AOT retrievals and mass measurements. The resulting points (without the circled/squared points) present a better correlation between the AOT versus PM2.5 mass and provide a correlation coefficient of $R^2 = 0.84$, slope = 0.011 and intercept = −0.011. For the PM10 comparison, we present a correlation coefficient of $R^2 = 0.67$, slope = 0.0017 and intercept = 0.056. Comparable to this PM10 correlation, *Smirnov et al.* [2000] reported a correlation coefficient of $R^2 = 0.71$, slope = 0.0036 and intercept = 0.082 for daily filters from a high-volume bulk sampler and daily average AOT measurements at 870nm from AERONET of the Saharan dust. They were able to improve the correlation to $R^2 = 0.93$ by presenting their 2.5-year data as 1-month averages.

3.2. Absorption Efficiency

[19] The absorption efficiency is an important variable connecting the aerosol absorption properties and the aerosol particle mass concentration, and can be used in chemical transport models to connect chemistry and optical properties. The absorption efficiency is measured from the exposed Nuclepore filter using an optical reflectance technique and the mass measurements (Martins et al., submitted manu-

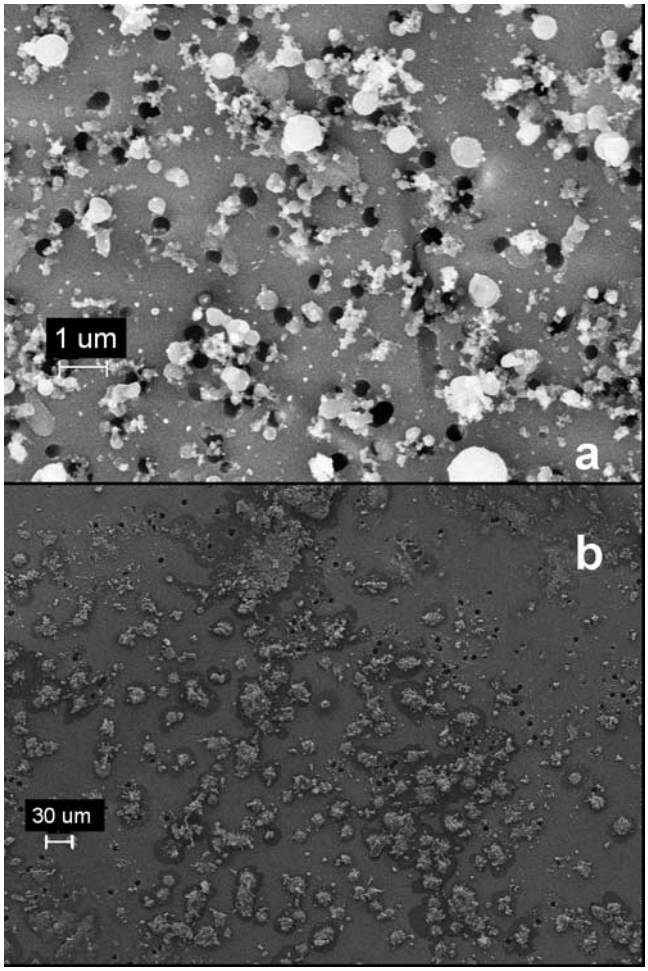

Figure 7. Scanning electron microscope image of (a) 10 March 2005 fine mode filter and (b) 12 March 2005 coarse mode filter. The scale in Figure 7a corresponds to 1 μm, and the scale in Figure 7b corresponds to 30 μm. The black circles shown are the filter pores whereas the particles are shown in white and gray tones.

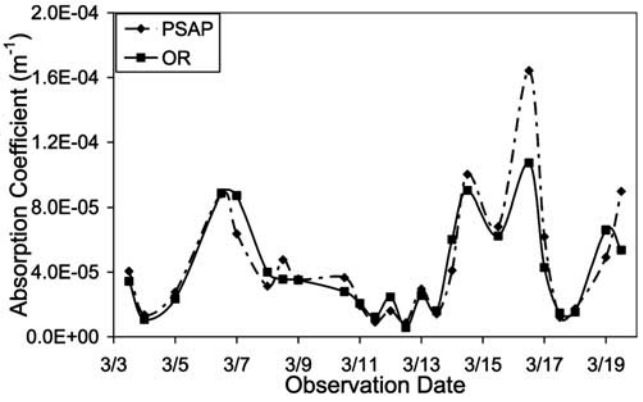

Figure 8. Comparison of absorption coefficient from the optical reflectance (OR) technique applied to the Nuclepore filters and the corresponding average PSAP results during the IOP.

script, 2007). The spectral dependence data provides important information on the average size of the absorbers, and some hints on the imaginary refractive index [*Martins et al.*, 1998]. In Figure 6a, the absorption efficiency of the coarse mode filters is shown as an average (black line) and one standard deviation (shaded) of the 35 filters that were collected during the IOP. A second line is plotted (gray) showing a λ^{-1} spectral dependence consistent with small absorbers, usually smaller than 0.2 μm diameter and flat imaginary refractive index, like black carbon [*Martins et al.*, 1998; *Bergstrom et al.*, 2002]. The absorption efficiency of the coarse mode has a much flatter spectral dependence than the λ^{-1} line, which is consistent with larger particles with flat refractive indices possibly representing large black carbon cluster aggregates or combinations between dust particles and black carbon [*Martins et al.*, 1998]. However, the fine mode filters absorption efficiency is very similar to the λ^{-1} model, as shown in Figure 6b. Departures from the λ^{-1} curve for small absorbing particles can be related to relatively fast changes in the imaginary component of the refractive index which is commonly observed in the short-wavelength visible and the UV for organic materials [*Chang and Charalampopoulos*, 1990; *Kirchstetter et al.*, 2004], nitrated or aromatic aerosols [*Jacobson*, 1999], or dust.

[20] The fine and coarse mode absorption efficiencies are compared side by side in Figure 6c. While the fine mode is a more efficient absorber in the UV and visible regions, in the near-IR, both modes are equally good absorbers, indicated by the overlapping error bars. Much of the incoming solar radiation is absorbed in this region of the spectrum, and since the coarse mode mass is much greater than that of the fine (Figures 1a and 1b), the large absorption by the coarse mode is significant and is rarely taken into account in climate studies.

[21] The typical fine and coarse particles collected in Xianghe during the IOP were observed by the use of a scanning electron microscope on sections of the filter. Pictures were taken of several representative filters with the scanning electron microscope at the NASA Goddard Space Flight Center in Greenbelt, MD. Figure 7a shows an example for the filter collected on 10 March, where the fine-mode filter shows a combination of spherical particles and aggregates of much smaller particles. The black circles represent the filter pores while the particles are pictured in shades of white and gray. The 1 μm scale on the bottom left corner indicates that all particles are smaller than 2.5 μm. The coarse mode filter SEM in Figure 7b shows large particles, probably composed of a combination of dust, black carbon, and organic material, from 12 March. The mixture between dust and black carbon could justify some of the absorption efficiency spectral dependence observed in Figure 6a.

[22] The absorption coefficient calculated from a combination of the OR and the mass concentration was compared to the University of Maryland's PSAP instrument, which was run in parallel with the filter sampling apparatus during the IOP. This comparison is shown in Figure 8. There is a better agreement between the two experimental techniques at lower values of the absorption coefficient, while the disparity between the data points widens at higher values, probably because of biases of the PSAP corrections for higher loading, and the excessive light attenuation allowed for those cases which could have produced transmittances down to 60%. At seven points the difference between the two measurements is greater than ±1E-05. The points where the OR measures a significantly greater absorption coefficient (7, 14, and 19 March) were all during the nighttime sampling period when the PSAP has difficulty taking continuous measurements (see below for discussion). The largest difference between points occurs over the whole day of 16 March ending on 17 March when there was heavy atmospheric loading based on Figure 2.

[23] Using the scattering coefficient from the University of Maryland's TSI three-wavelength Nephelometer, the SSA (ω_0) was calculated for both the filter OR and the PSAP results. While the absorption coefficient can be derived from the OR measurement at any wavelength from 350 to 2500 μm, the Nephelometer only measures at 450, 550 and 700 nm. The ω_0 was calculated at these three wavelengths and is shown in Figure 9. The PSAP only operates at one wavelength, 574 nm. The filter OR ω_0 calculation at 550 nm is then compared with that from the PSAP (extrapolated from 574 nm to 550 nm), and AERONET at 441 nm and 673 nm in Figure 10. The ω_0 from AERONET is an inversion product derived from almucantar

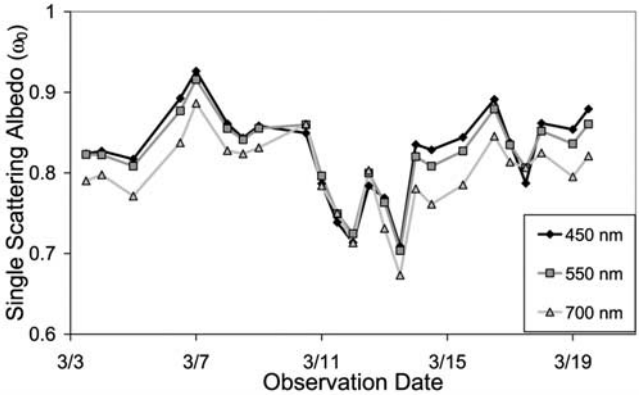

Figure 9. Single scattering albedo (ω_0) from optical reflectance combined with the Nephelometer scattering coefficient at the three operating wavelengths: 450, 550, and 700 nm.

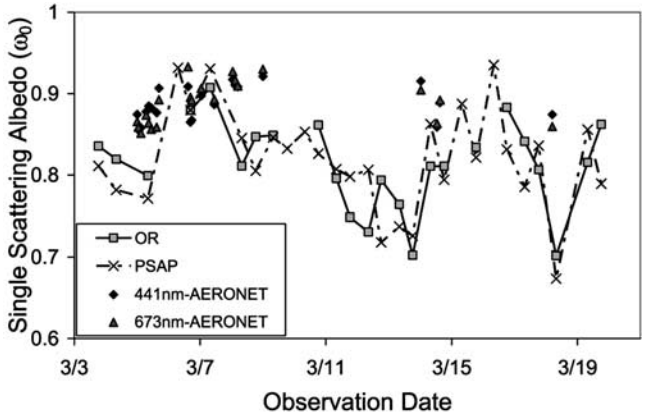

Figure 10. Single scattering albedo from AERONET and a combination of the scattering coefficient from the Nephelometer at 550 nm with optical reflectance and PSAP results.

and principle plane measurements, not direct Sun measurements, and hence has fewer data points. To allow for some comparison, all data points during this time period are shown, not just daily averages. The data shows that AERONET's ω_0 is higher than that obtained from the ground-based measurements. AERONET's inversion-based calculation would be influenced by aerosol layers aloft or possibly by hydration of the ambient aerosol particles, neither of which would affect the dry filter samples collected at the surface and analyzed in the lab. The range of ω_0 during the IOP is from 0.70 to 0.94, and the variation can be explained by the passage of cold fronts, wind direction and wind speed, as shown by *C. Li et al.* [2007].

[24] Since the PSAP and Nephelometer instruments offer higher temporal resolution than OR, we examined the diurnal cycle of ω_0 to determine whether or not the larger averaging time would impact the findings. In Figure 11, the daily cycle of ω_0 is shown with one standard deviation at each data point. Also plotted on Figure 11 is the number of data points that contributed to each average from the PSAP instrument. Since the PSAP is a filter-based instrument using paper filters, the absorption measurement is only valid until a certain threshold of loading on the filter, at which time the filter must be replaced. In the case when an operator was not able to change the filter and the threshold was breached, that data removed from the data set. The number of data points that contributed to each average point gives us an idea of the certainty of the measurement. The diurnal cycle of ω_0 shows two minimum values, one during the morning and one in the evening. The morning minimum occurs at a time when home heating systems are fired up and cooking for the day begins. Both minima can be attributed to rush hour commutes as well.

4. Conclusions

[25] Nuclepore filters were collected in Xianghe, China for the first 5 months of 2005. Mass concentration measurements derived from the filters indicate substantial atmospheric concentrations of both PM2.5 and PM10. The ground-based mass concentration measurements compare favorably with AERONET AOT and size distribution retrievals in cases of vertical homogeneity as observed by the lidar data, which allows for converting remotely sensed AOT to mass concentration. The spectral absorption efficiency was measured for the coarse and fine mode filters using an optical reflectance technique. The fine mode compared favorably to a λ^{-1} model while the coarse mode exhibited much flatter spectral dependence, consistent with large particle models. The coarse mode absorption efficiency in the NIR region was determined to be similar in strength to the fine mode. This implies very strong absorption by the coarse mode, considering the sizable mass of coarse particles in the atmosphere, which is important for the energy balance of the atmosphere, considering that much of the incoming solar radiation is present in this region of the spectrum. The substantial absorption observed by the coarse mode during this experiment is significant and should be emphasized in future studies as it is rarely taken into account in climate studies.

[26] The absorption coefficient was calculated at 550 nm from the OR technique and compared to a colocated PSAP. At low to moderate levels of absorption, the two measurement techniques compared very well, while the disparity increased at higher loading levels, probably because of the optical artifacts in the PSAP as well as few nighttime measurements. The absorption coefficients were combined with the scattering coefficient from a colocated Nephelometer

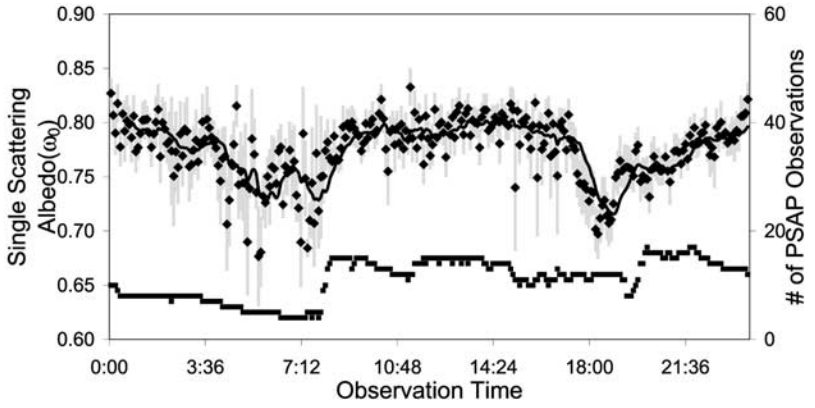

Figure 11. Diurnal cycle of single scattering albedo from PSAP and Nephelometer (diamonds) with error bars (light gray) and the number of data points from PSAP contributing to the average (squares).

to produce ω_0. Both ground-based measurements produced a lower ω_0 than AERONET, implying higher concentration of absorbers near the surface than aloft, or other intrinsic differences between the dry filter samples and the ambient measurements collected by AERONET. Such information is important to compute the temperature profile due to diabatic heating by the aerosols. In the future, we plan to conduct more experiments using either airborne or balloon-borne instruments to better resolve the vertical profile of ω_0.

[27] **Acknowledgments.** The EAST-AIRE project was supported by the NASA Radiation Science Program (NNG04GE79G), the National Science Foundation (ATM0412040, ATM425069), the National Science Foundation of China (40250120071), and the 973 Aerosol Initiative sponsored by the Chinese Ministry of Science and Technology. The absorption measurements were supported by the NASA Radiation Science Program. The authors would like to thank Jacob Kleidman for his filter/OR laboratory assistance and Debbie Thomas from NASA GSFC code 541.0 for her support on the SEM laboratory analysis.

References

Bergin, M. H., et al. (2001), Aerosol radiative, physical, and chemical properties in Beijing during June 1999, *J. Geophys. Res.*, *106*(D16), 17,969–17,980.

Bergstrom, R. W., P. B. Russell, and P. Hignett (2002), Wavelength dependence of the absorption of black carbon particles: Predictions and results from the TARFOX experiment and implications for the aerosol single scattering albedo, *J. Atmos. Sci.*, *59*, 567–577.

Bond, T. C., T. L. Anderson, and D. Campbell (1999), Calibration and intercomparison of filter-based measurements of visible light absorption by aerosols, *Aerosol Sci. Technol.*, *30*, 582–600.

Chang, H., and T. T. Charalampopoulos (1990), Determination of the wavelength dependence of refractive indices of flame soot, *Proc. R. Soc. London, Ser. A*, *430*, 577–591.

Chu, D. A., Y. J. Kaufman, C. Ichoku, L. A. Remer, D. Tanré, and B. N. Holben (2002), Validation of MODIS aerosol optical depth retrieval over land, *Geophys. Res. Lett.*, *29*(12), 8007, doi:10.1029/2001GL013205.

Clarke, A. D. (1982), Effects of filter internal reflection coefficient of light absorption measurements made using the integrating plate method, *Appl. Opt.*, *21*, 3021–3031.

Coakley, J. A., and P. Chylek (1975), The two-stream approximation in radiative transfer: Including the angle of incident radiation, *J. Atmos. Sci.*, *32*(2), 409–418.

Hansen, A. D. A., H. Rosen, and T. Novakov (1982), Real-time measurement of the absorption coefficient of aerosol particles, *Appl. Opt.*, *21*, 3060–3062.

Holben, B. N., et al. (1998), AERONET—A federated instrument network and data archive for aerosol characterization, *Remote Sens. Environ.*, *661*(1), 1–16.

Hopke, P. K., Y. Xie, T. Raunemaa, S. Biegalski, S. Landsberger, W. Maenhaut, P. Artaxo, and D. Cohen (1997), Characterization of the Gent Stacked Filter Unit PM10 sampler, *Aerosol Sci. Technol.*, *27*, 726–735.

Huebert, B. J., T. Bates, P. B. Russell, G. Shi, Y. J. Kim, K. Kawamura, G. Carmichael, and T. Nakajima (2003), An overview of ACE-Asia: Strategies for quantifying the relationships between Asian aerosols and their climatic impacts, *J. Geophys. Res.*, *108*(D23), 8633, doi:10.1029/2003JD003550.

Ichoku, C., D. A. Chu, S. Mattoo, Y. J. Kaufman, L. A. Remer, D. Tanré, I. Slutsker, and B. N. Holben (2002), A spatio-temporal approach for global validation and analysis of MODIS aerosol products, *Geophys. Res. Lett.*, *29*(12), 8006, doi:10.1029/2001GL013206.

Intergovernmental Panel on Climate Change (2001), *Climate Change 2001: The Scientific Basis*, edited by J. T. Houghton et al., 896 pp., Cambridge Univ. Press, New York.

Jacobson, M. Z. (1999), Isolating nitrated and aromatic aerosols and nitrated aromatic gases as sources of ultraviolet light absorption, *J. Geophys. Res.*, *104*(D3), 3527–3542.

Jacobson, M. Z. (2000), A physically-based treatment of elemental carbon optics: Implications for global direct forcing of aerosols, *Geophys. Res. Lett.*, *27*, 217–220.

John, W., S. Hering, G. Reischl, G. Sasaki, and S. Goren (1983), Characteristics of Nuclepore filters with large pore size, II. Filtration properties, *Atmos. Environ.*, *17*, 373–382.

Kaufman, Y. J., D. Tanre, L. A. Remer, E. F. Vermote, D. A. Chu, and B. N. Holben (1997), Operational remote sensing of tropospheric aerosol over land from EOS moderate resolution imaging spectroradiometer, *J. Geophys. Res.*, *102*, 17,051–17,067.

Kindel, B. C., Z. Qu, and A. F. H. Goetz (2001), Direct solar spectral irradiance and transmittance measurements from 350 to 2500 nm, *Appl. Opt.*, *40*(21), 3483–3494.

Kirchstetter, T. W., T. Novakov, and P. V. Hobbs (2004), Evidence that the spectral dependence of light absorption by aerosols is affected by organic carbon, *J. Geophys. Res.*, *109*, D21208, doi:10.1029/2004JD004999.

Li, C., L. T. Marufu, R. R. Dickerson, Z. Li, T. Wen, Y. Wang, P. Wang, H. Chen, and J. W. Stehr (2007), In situ measurements of trace gases and aerosol optical properties at a rural site in northern China during East Asian Study of Tropospheric Aerosols: An International Regional Experiment 2005, *J. Geophys. Res.*, *112*, D22S04, doi:10.1029/2006JD007592.

Li, Z., et al. (2007), Aerosol optical properties and their radiative effects in northern China, *J. Geophys. Res.*, *112*, D22S01, doi:10.1029/2006JD007382.

Lin, C. I., M. Baker, and R. J. Charlson (1973), Absorption coefficient of atmospheric aerosol: A method for measurement, *Appl. Opt.*, *12*(6), 1356–1363.

Ma, C.-J., M. Kasahara, R. Holler, and T. Kamiya (2001), Characteristics of single particles sampled in Japan during the Asian dust-storm period, *Atmos. Environ.*, *35*, 2707–2714.

Martins, J. V., P. Artaxo, C. Liousse, J. S. Reid, P. V. Hobbs, and Y. J. Kaufman (1998), Effects of black carbon content, particle size, and mixing on light absorption by aerosols from biomass burning in Brazil, *J. Geophys. Res.*, *103*(D24), 32,041–32,050.

Ning, D., L. Zhong, and Y. Chung (1996), Aerosol size distribution and elemental composition in urban areas of northern China, *Atmos. Environ.*, *30*, 2355–2362.

Reid, J. S., P. V. Hobbs, C. Liousse, J. V. Martins, R. E. Weiss, and T. F. Eck (1998), Comparison of techniques for measuring shortwave absorption and black carbon content of aerosols from biomass burning in Brazil, *J. Geophys. Res.*, *103*(D24), 32,031–32,040.

Remer, L. A., et al. (2002), Validation of MODIS aerosol retrieval over ocean, *Geophys. Res. Lett.*, *29*(12), 8008, doi:10.1029/2001GL013204.

Shi, Z., L. Shao, T. P. Jones, A. G. Whittaker, S. Lu, K. A. Berube, T. He, and R. J. Richards (2003), Characterization of airborne individual particles collected in an urban area, a satellite city and a clean air area in Beijing, 2001, *Atmos. Environ.*, *37*, 4097–4108.

Smirnov, A., B. N. Holben, D. Savoie, J. M. Prospero, Y. J. Kaufman, D. Tanre, T. F. Eck, and I. Slutsker (2000), Relationship between column aerosol optical thickness and in situ ground based dust concentrations over Barbados, *Geophys. Res. Lett.*, *27*, 1643–1646.

Virkkula, A., N. C. Ahlquist, D. S. Covert, W. P. Arnott, P. J. Sheridan, P. K. Quinn, and D. J. Coffman (2005), Modification, calibration and a field test of an instrument for measuring light absorption by particles, *Aerosol Sci. Technol.*, *39*, 68–83.

Weiss, R., and A. Waggoner (1984), Aerosol optical absorption: Accuracy of filter measurement by comparison with in-situ extinction, in *Aerosols*, edited by B. Liu, D. Pui, and H. Fissan, pp. 397–400, Elsevier, New York.

Winker, D. M., J. R. Pelon, and M. P. McCormick (2003), The CALIPSO mission: Spaceborne lidar for observation of aerosols and clouds, *Proc. SPIE Int. Soc. Opt. Eng.*, *4893*, 1–11.

Yamasoe, M. A., P. Artaxo, A. H. Miguel, and A. G. Allen (2000), Chemical composition of aerosol particles from direct emissions of vegetation fires in the Amazon Basin: Water-soluble species and trace elements, *Atmos. Environ.*, *34*, 1641–1653.

Ye, B., X. Ji, H. Yang, X. Yao, C. K. Chan, S. H. Cadle, T. Chan, and P. A. Mulawa (2003), Concentration and chemical composition of PM2.5 in Shanghai for a 1-year period, *Atmos. Environ.*, *37*, 499–510.

Zhao, F., and Z. Li (2007), Estimation of aerosol single scattering albedo from solar direct spectral radiance and total broadband irradiances measured in China, *J. Geophys. Res.*, *112*, D22S03, doi:10.1029/2006JD007384.

Zwally, H. J., et al. (2002), ICESat's laser measurements of polar ice, atmosphere, ocean, and land, *J. Geodyn.*, *34*, 405–445.

Z. Chaudhry, R. R. Dickerson, C. Li, and Z. Li, Department of Atmospheric and Oceanic Science and the Earth System Science Interdisciplinary Center, University of Maryland, College Park, MD 20742, USA. (zahra@atmos.umd.edu)

H. Chen, P. Wang, and T. Wen, Institute of Atmospheric Physics, Chinese Academy of Sciences, Beijing 100029, China.

J. V. Martins, Department of Physics and Joint Center for Earth Systems and Technology, University of Maryland, Baltimore County, Baltimore, MD 21250, USA.

S.-C. Tsay, NASA Goddard Space Flight Center, Greenbelt, MD 20771, USA.